# SESSION 6B

# ELECTROSTATIC PRECIPITATION MODEL DEVELOPMENT AND PILOT SCALE RESEARCH

# PRELEC: A MATHEMATICAL MODEL OF ELECTROSTATIC PRECIPITATION

L. Cañadas
B. Navarrete
L. Salvador
A. Rodríguez-Aragonés
Dept. Ingeniería Química y Ambiental
Escuela Superior de Ingenieros Industriales
Avd. Reina Mercedes, s/n
41012-SEVILLA, SPAIN

## Abstract

This paper is the first presentation of a model designed to characterize the performance of plate-type electrostatic precipitators (ESP). PRELEC is a rigorously Deutschian model, completely theoretically-derived, that avoids the use of empirical estimations in its calculations. In the present version, those estimations related with non-ideal effects are not considered.

PRELEC calculates electric fields, based on the applied voltage wave, including the effects of ionic and particulate space-charge. It is able to simulate two possible types of ESP energization: full-wave rectified current and pulse generation. It also allows the transient evolution of electrical conditions inside the ESP during the rapping intervals to be analyzed, taking into account the dust build-up influence. The model predictions show good agreement with experimental measurements taken at two ESPs of Spanish Power Plants under several operational conditions, including different dust characteristics, very high resistivity ashes, operation before and after the installation of a flue gas conditioning plant, and the use of rectified current and pulse energization. PRELEC predictions are also compared with those obtained from Version 3 of EPA/SRI model.

## Introduction

The wide range of operational conditions in which ESPs are involved, rising from low to high dust resistivity or dust concentration, the different energization techniques applied, and the need for more insight into fundamental processes occurring during electrostatic precipitation, justify any effort made to improve the tools which could be used to analyze ESPs performance, mainly the ESP mathematical models.

Although several high level models have been proposed in recent last years, and some of them have shown very good behaviour when simulating determined operational situations, at present there is no model capable of simulating all possible real situations concerning ESPs utilization.

Thus, Version 3 of the EPA/SRI model (1), probably the most extensively evaluated and used model, presents some limitations concerning the treatment of the particle space-charge, the electrical behaviour of the dust layer and the energization system. Other models, like the ADA ESP (2), are designed to simulate situations with very high inlet dust concentrations, but only under the low resistivity conditions resulting from dry scrubbing desulfurization processes. PRELEC represents an effort to develop a general purpose ESP model based on a completely theoretical formulation, that considers, in an open way, all the relevant aspects which influence ESP performance. PRELEC avoids the use of empirical assumptions or approximations, not including parameters which could not be directly evaluated from standard measurements or fundamental equations. So, this first version of PRELEC does not incorporate the treatment of the non-ideal factors commonly used due to the present uncertainty associated to their estimation. Nevertheless, it includes a rigorous evaluation of all the local physical magnitudes which describe, according to the state-of-the-art, the phenomena taking place inside an ESP. The model can even simulate two different types of ESP energization, a full-wave rectified current and over-imposed pulse generation, integrating the electrical wave form during precipitation, and it can consider the electrical effect of the dust cake. These capabilities also enable the model to simulate the transient behaviour of an electrical section between two rapping intervals.

## General Statement of PRELEC Model

The approach taken in the PRELEC model development was to configure a rigorously Deutschian model based on a consistent set of fundamental equations, including those related to the electric field in plate-type precipitators, the current-voltage characteristic, the effect of ion and particle space charges on the field distribution, the charging process, the particle motion, and the growth and behaviour of the dust layer. This set of fundamental equations has been directly derived from the theoretical background of electrostatic precipitation, perfectly summarized in the treatise by J. Böhm (3). In the PRELEC model, as in the EPA/SRI and the ADA ESP models, the Deutsch equation is applied to narrow particle size bands in short length increments of the ESP. Each length increment used by PRELEC contains a centered discharge electrode, assuming that wires are uniformly distributed along the ESP length. As can be seen in Figure 1, PRELEC input data only include the applied voltage wave form, the current intensity being obtained by calculation of the effective electric field distribution within the ESP. The model algorithm uses iterative technique to solve the constitutive equations until self consistency is assured by mathematical convergence of calculated parameters in each element, as the logic diagram of Figure 1 shows.

PRELEC considers the internal T/R voltage wave form and the electric field shape factors to evaluate the charge acquired by particles, and takes into account both the ionic and particle space-charges, the voltage drop across the dust layer, and also the modification of the electric wave form due to the capacitance of the electrode system (4). So, in its formulation the model explicitly takes into account the effect of dust concentration and dust resistivity on the precipitation process.

The model allows a transient analysis during the rapping intervals in the whole ESP, by dividing these intervals in several time periods defined by the user, which are independently evaluated, obtaining the growth pattern of the dust layer and the time evolution of the rest of the variables. This special feature of PRELEC model has been designed in order to allow the study and optimization of the rapping intervals and the analysis of electrical behaviour of dust layers looking at the future objective of simulating back corona and dust reentrainment.

## Description of the Mathematical Model

### *The precipitation variables*

The PRELEC model uses the following fundamental variables to represent the physical phenomena of electrostatic precipitation:

| | | |
|---|---|---|
| $\mathbf{U}$ | : | Applied voltage. |
| $\mathbf{U_i}$ | : | Ionizing voltage. |
| $\mathbf{z}$ | : | Radius of active zone. |
| $\mathbf{i_S}$ | : | Current intensity arriving at the plates. |
| $\mathbf{U_p}$ | : | Voltage induced by particle space charge. |
| $\beta_i$ | : | Relative particle charge of each particle size. |
| $\mathbf{C_i}$ | : | Mass concentration of each particle size. |
| $\mathbf{w_i}$ | : | Migration velocity of each particle size |
| $\tau$ | : | Dust layer thickness. |
| $\rho_v$ | : | Particle layer resistivity. |
| $\mathbf{U_v}$ | : | Voltage drop across deposit layer. |

All these variables are substantially interdependent, and consequently their coupled values must constitue a consistent set in each ESP increment.

### *The fundamental equations*

In the following, the equations describing the main processes which take place in an ESP will be presented in the form in which they are used by the PRELEC model:

**1.** The electrical field in a plate–type ESP can be written as:

$$E = \frac{\pi\ U}{2\ R\ F}\ X \tag{1}$$

where R represents the distance between plate and discharge electrode, F is a configuration factor depending on the internal ESP geometry, and X is the shape factor depending on the relative position considered.
This equation allows the evaluation of the resultant of the electric field in a discrete position of a defined ESP geometry as an explicit function of applied voltage.

2. The charging process is defined by means of the relative particle charges. The gradual charging of one particle by a combination of ion bombardment and ion diffusion, as the gas stream carries it through the working space of the ESP, is expressed by the following differential equation:

$$d\beta = [\![ \frac{b}{R^2} [1 - \beta \frac{U_m X_m}{UX}]^2 \cdot \frac{UX}{U_m X_m} + \\ + \frac{2FV_{ef}}{\pi X R(U_m X_m)} \exp[ - \beta \frac{\pi \chi e D_p (U_m X_m)}{4RFkT} ]]\!] U_i \, dt \tag{2}$$

This equation contains the term UX which is a complex time dependent periodic function related to the voltage wave form and with the periodicity of the shape factor. PRELEC considers the ESP energized by an unfiltered full-wave rectified current as internal T/R wave form. From this baseline PRELEC estimates the voltage waves modification by the capacitive effect of the ESP and it is also able to overimpose voltage pulses with a value, duration and frecuency defined by the user.

3. The current-voltage characteristic in an ESP increment can be represented by:

$$i_s = \frac{4}{9} k \frac{b}{R^2} B \frac{(\overline{U} - U_p)}{(\mu F)} U_i \tag{3}$$

In this equation B means the current attenuation due to the charge captured by particles, which is determined by a balance of electrical charge in the precipitation element.
The application of eq. 3 to all the length increments in which the ESP is divided leads to the local evolution of the ionic current along the ESP.

4. The particles motion to the collecting plates is obtained from a balance of the forces acting on each charged particle: basically the electric force and the resistance of the gas flow. Assuming motion on the stokesian domain, the fractional drift velocity can be expressed by:

$$w_p = \frac{\pi^2}{12} \frac{\epsilon_0 \epsilon_1 \chi (U_m X_m)(U_s X_v)}{R^2 F^2 \eta_p} \beta D_p \tag{4}$$

The resulting migration velocity is directly applied to obtain the decrease in particle concentration and also the evolution of dust layer thickness.

5. A simple mass balance performed in the precipitation element constitutes the equation governing dust layer growth.

$$d\tau = \frac{C}{\rho_m} w \, dt \tag{5}$$

So, applying Ohm's law, the voltage drop across the dust layer is:

$$U_v = \rho_v h_v \tau \tag{6}$$

Developing eq. 5 and 6, it is possible to find the following relationships describing the formation of the deposit layer:

$$\tau = \frac{U}{\rho_v\, h_v}\,[1 - \exp(-\frac{t}{t_u})] \tag{7}$$

Where $t_u$ is the relaxation constant of the deposit formation process given by:

$$t_u = \frac{6\,\rho_m\, R\,(\mu F)\,\mu_G}{C\,\rho_v\, h_v\, X_v \left( \sum_i (ne)_{smE_i} \frac{\beta_i}{D_{p_i}} x_i \right)} \tag{8}$$

Eq. 6 and 8 make possible the calculation of voltage drop due to the deposit layer, which may represent an important fraction of applied voltage when the ash resistivity is high.

6. The voltage induced by the particles space–charge also represents a loss in the applied voltage reducing the amount of generated ions. This voltage, assuming that R >>r, can be evaluated by:

$$U_p = \frac{\rho_p\, R^2}{2\epsilon_0\epsilon_1} \tag{9}$$

where the density of the particle space–charge, $\rho_p$, can be expressed by:

$$\rho_p = \frac{3\pi\,\epsilon_0\,\epsilon_1\,\chi\,(U_m X_m)}{R\,(\mu F)\,\rho_c}\, C \int_{z=0}^{1} \frac{\beta}{D_p}\, dz \tag{10}$$

The resolution of these basic equations in each length increment of the ESP allows the PRELEC model to describe the electrostatic precipitation process. The solution procedure applied to solve this highly coupled set of equations uses an iterative algorithm which achieves consistent values for all the involved variables. After this, as showed in Figure 1, the Deustch equation is applied to each particle size band in order to obtain the collecting efficiency, the reduced dust concentration and the new particle size distribution at the ESP element outlet.

## Experimental Measurements and Model Comparison

The validation process of the PRELEC model has been planned in two ways: direct comparison between performance of full–scale ESPs and model predictions, and also comparison between PRELEC and Version 3 of the EPA/SRI model results simulating identical real situations. The field data have been taken from the ESPs of two Spanish Power Plants whose main characteristics are presented in Table 1. For both ESPs, measurements under very different operating conditions have been available, so the study case series include:

1. ESP No.1 only energized with rectified current, collecting ashes from local coal.
2. ESP No.1 operating with pulse energization in two electric sections and $SO_3$ gas conditioning.

3. ESP No.2 collecting ashes from a South African coal.
4. ESP No.2 collecting ashes from an American coal.

The mean operating conditions for each series of study cases are summarized in Table 2 whose representative figures are the average values for all the individual conditions. Also shown in Table 2 are the average efficiencies obtained by PRELEC and EPA/SRI model for each series. Two kind of EPA/SRI predictions have been considered, according to the used input data and model capabilities. The indicated EPA/SRI analysis results have been obtained imposing the measured voltages and current intensities on the model, whereas for the EPA/SRI design results only the voltages have been specified and the current densities are evaluated by the model. All the presented EPA/SRI results have been calculated using non-ideal effects of 10% sneakage-reentrainment and 25% standard deviation for the gas velocity distribution (5).

A more detailed comparison between model predictions and experimental measurements of ESP efficiency is shown in Figure 2 which presents the results of all the individual study cases.

The average results presented in Table 2 indicate that PRELEC model efficiency predictions obtain good agreement with measured values in all the validation series, and that some important differences exist between the two models performance. Both models have similar behaviour when simulating the operation of ESP No.2 (case series 3 and 4). Only some efficiency overestimation is produced, slightly greater for the EPA/SRI model. In this sense, it is important to point out the fact that all the EPA/SRI design runs achieve lower operational voltages than specified because the model estimates that the breakdown field near the plates is exceeded. A more informative comparison between models is offered by the results of ESP No.1 simulation (case series 1 and 2), where the advantages obtained by PRELEC model are also more clearly stated. Looking at PRELEC results in these series, a slight efficiency underestimation is evident, but predictions achieve quite a good concordance with measured values and similar behaviour of the model is obtained in the two series. This markedly contrasts with the differences showed by EPA/SRI model runs. The EPA/SRI model answers the high efficiency cases of serie 2 with quite a low efficiency prediction when the model operates in the analysis mode, using as input data the continuous baseline voltages existing in the ESP sections and the total current density obtained by both the baseline voltages and the over imposed voltage pulses. In addition, the EPA/SRI analysis runs for series 1 prove this model to be un-applicable to predict collection efficiencies under the low voltage and very low current conditions existing in those cases, where the operation of the ESP was strongly influenced by the existence of a cohesive and highly resistive dust layer over the collecting plates with an average thickness of 3 to 4 mm. This reason justifies the high overestimation (4 points) obtained by the EPA/SRI design runs on the efficiency of series 1 cases. On the other hand, the EPA/SRI model working in the design mode predicts a low ESP efficiency in the cases of series 2 as a consequence of its impossibility to account for the improvement in precipitation due to voltage pulses. However, the predicted efficiency by EPA/SRI model agrees with the results of PRELEC model when it runs without considering pulse energization. In this case, the averaged efficiency obtained by PRELEC is 99,1% instead the 99,0% predicted by EPA/SRI model.

Another important aspect of model validation is the comparison between measured and predicted ESP current densities. At the end of Table 2 the average values of this variable extended over the whole ESP are presented. In all cases the predicted current density is higher than the measured one, but PRELEC results are relatively close to experimental values, more than those obtained by the EPA/SRI model design runs. The important differences between both models are not only quantitative but also qualitative, because the EPA/SRI design results present flat profiles of current density inside the ESP, whereas PRELEC results approximately fit the shape of the measured profiles.

## Sensitivity Analysis of the Model

The PRELEC model is able to account for the explicit influence of dust resistivity, dust concentration, and dust layer thickness in the precipitation process and its results faithfully reproduce the expected trends of ESP performance when the value of these parameters is changed.

Figure 3 shows the predicted evolution of the ESP penetration when the dust resistivity increases, maintaining invariable the rest of the model input data. The obtained currents indicate that the model is only sensitive to resistivity values larger than $10^{11}$, due to the increase in voltage drop through the dust layer which produces the consequent decrease in the net voltage existing for precipitation. As can be seen in Figure 2, the qualitative effect of dust resistivity is similar for cases of high and low collection efficiency, although the absolute increase in penetration grows as the ESP efficiency decreases. The effect represented in Figure 2 only accounts for the net influence of resistivity value considering that the applied voltages are not modified. However, at very high dust resistivities the voltages should be reduced in order to avoid the on-set of back corona yielding higher penetration figures than presented. The sensitivity to dust resistivity is directly related to the thickness of the dust layer existing over the collecting plates, which depends on the rapping cycles, the dust adherence, and the effectiveness of the rapping system. In Figure 3 plots of ESP efficiency versus dust resistivity using different permanent layer thicknesses are presented, showing the cumulative effect of both factors. It has to be noted that a similar increase in layer thickness has a lower relative influence as the layer grows, derived from the gradual decrease in current density associated to this process.

Inlet dust concentration to the ESP is another very interesting factor associated to electrostatic precipitation. Dust concentration inside the ESP affects the electrostatic process in various ways. First, particles adsorb electrical charge and create a distribution of particle space-charge which opposes to the corona current flow from the wires. When the dust load grows the particle space-charge also increases and an equilibrium needs to be reached, imposing a lower charging rate of the particles and even, at very high mass-loadins, stopping the corona discharge. The results obtained by PRELEC model, using input data taken from different selected cases, indicate that inlet dust concentrations as low as 10 g/Nm$^3$, affect ESP performance showing important increases is ESP penetration when the dust load exceeds this value. Figure 4 presents the obtained trends in two very different situations, one corresponding to a case of series 1 and other to a case of series 3, where the shape of the curves is approximately the same in a log-plot.

In addition to the quenching of the corona discharge in the first wires of an ESP, higher dust loads also produce a modification in the electric charge balance inside the ESP which leads to a reduction of the current arriving at the plates, in parallel with an increase in the growth rate of the dust layer. The current reduction appears as the predominant effect and consequently the voltage drop through the deposit layer tends to decrease in the first sections of the ESP. Both factors, the corona shielding and the modification of the global electric conditions, are more significant with smaller particle sizes.

The study of transient evolution of an electrical section offers results like those presented in Figure 6, this figure shows the current density and the dust layer thickness distributions along the field 1 of ESP No.2 obtained at different times after the last rapping. In this case a dust layer of 1 mm thickness remaining after rapping was imposed and the inlet dust concentration to the ESP was 13,3 $g/Nm^3$. Results indicate a fast growth of the dust layer over the first elements of the electrical section, producing a considerable fall of the corresponding current densities. The different rate of dust precipitation from the section inlet to the outlet determines the uneven layer distribution predicted by the model, with maximum thickness always obtained at the first precipitation element.

The shape of current densities profiles also indicates the balance between the two mechanisms of current flow. Looking at the curve for 240 s, a minimum near the field center is clearly shown. Current density before the minimum is dominated by the charge carried by particles, leading to the high current densities existing at the field inlet. While the rise in current density obtained after the minimum is due to the increase in ionic current produced by the dust load reduction in the working space.

The estimated penetration for this case only varies with time from 3,8 % at 240 s to 4,1% at 1200 s, although important modifications on the internal electric behavior are produced.

## Further Developments

Although results of version 1 of PRELEC model shows quite a good concordance with experimental results, it has some conceptual limitations which should be solved by additional work. This additional work has to be focussed in two ways: first, extending the actual model abilities to cover more ESP features, like the treatment of ESP energization by voltage wave forms other than the full wave rectified current, with and without pulse generation, trying to include intermitent energization and filtered d.c. fields, and allowing the use of non-symetric ESP elements or ESP elements composed of more than one discharge electrode, in order to make a totally representative geometric description of actual ESPs. Secondly, including some important aspects not yet considered by the model, such as the non-ideal processes concerning uneven gas distribution, gas sneakage and rapping and non-rapping reentrainment, and also non-ideal electric behaviour like the on-set and development of back corona.

The first improvement steps should involve a more detailed mathematical structure, whereas the second ones should also need the incorporation of well defined accurate empirical relationships and, probably results from in-depth insights into the dust cake structure and dust dislodgement process in conexion with rapping.

## Conclusions

The PRELEC model has proved its ability to make accurate predictions of ESP performance under a wide range of operating conditions, presenting similar good behaviour in cases of high and low overall efficiency, which involve high to very high resistivity ashes, different energization systems and also quite high inlet mass–loadings.

The model results also compare favorably with the outputs of Version 3 of the EPA/SRI model simulating the same situations, taking a special advantage in those cases where the ESP efficiency is conditioned by low voltages and very low current densities, due to the presence of a thick highly–resistive dust layer over the collecting plates, or the ESP is energized by voltage pulses.

The PRELEC model also reproduces the expected general trends of electrostatic precipitation when changes in ash resistivity, deposit thickness or dust concentration are produced, as a consequence of its explicit consideration of the voltage drop through the dust layer and the effect of particulate space–charge.

The model has been designed with the capability of making transient studies of ESP operation and performance during the rapping cycles, allowing the user to specify the time increments to be considered. Using this model feature detailed analysis of the electrical conditions evolution are obtained in order to serve as a specialized tool for new developments.

## References


1. M.G. Faulkner, and J.L. DuBard. *A Mathematical Model of Electrostatic Precipitation (Revision 3). Volume I: Modeling and Programming. Volume II: User's Manual.* EPA–600/7–84–069. August, 1984.

2. D.B. Holstein, D.E. Rugg, and M.D. Durham, "Development of an ESP Model for Dry Scrubbing Applications", EPRI Nith Particulate Control Symposium, Williamsburg, Virginia (October 1991).

3. J. Böhm. *Electrostatic Precipitators*. New York, N.Y.: Elsevier, 1982

4. P.A. Lawless, N. Plaks, and R.F. Altman, "Modeling Wave Effects in ESPs: The algorithm in ESPM and ESPVI", EPRI Nith Particulate Control Symposium, Williamsburg, Virginia (October 1991).

5. J.L. DuBard and R.S. Dahlin. *Precipitator Performance Estimation Procedure*. Palo Alto, Calif.: EPRI, February 1987. CS–5040.

## Notation

| | |
|---|---|
| b | Ion mobility |
| e | Elementary charge |
| $h_v$ | Current density in deposit layer |
| $i_S$ | Specific current (per unit length of discharge electrode) |
| k | Boltzmann constant |
| $(ne)_{smE}$ | Max. particle charge attainable by ion bombardment |
| t | Time |
| $t_u$ | Relaxation constant of deposit formation process |
| w | Migration velocity |
| z | Radius of active zone |
| B | Current attenuation coefficient |
| C | Particle concentration |
| $D_p$ | Particle diameter |
| E | Electric field strength |
| F | Electrode-system configuration factor |
| R | Distance between plates and discharge electrodes |
| T | Gas temperature |
| U | Voltage |
| $\bar{U}$ | Net available voltage |
| $U_i$ | Ionizing voltage |
| $U_m$ | Peak voltage value |
| $U_p$ | Voltage induced by particle space-charge |
| $U_s$ | Mean voltage value |
| $U_v$ | Voltage drop across deposit layer |
| $V_{ef}$ | Effective velocity of gas molecules |
| $\beta$ | Relative particle charge |
| $\varepsilon_0$ | Permittivity of a vacuum |
| $\varepsilon_1$ | Relative permitivity of gas |
| $\mu$ | Collecting capacity of plates |
| $\mu_G$ | Gas viscosity |
| $\rho_C$ | Specific gravity of particles |
| $\rho_m$ | Specific gravity of dust layer |
| $\rho_p$ | Density of particle space-charge |
| $\rho_v$ | Particle layer resistivity |
| $\tau$ | Dust layer thickness |
| $\chi$ | Charging coefficient |
| X | Shape factor of the electrostatic field |
| $X_m$ | Max. value of field shape factor |
| $X_v$ | Shape factor of electrostatic field in the deposit layer |

| | ESP No.1 | ESP No.2 |
|---|---|---|
| Number of chambers | 2 | 4 |
| Electrical sections per chamber | 4 | 5 |
| Gas passages per chamber | 30 | 42 |
| Plate spacing (mm) | 400 | 300 |
| Effective heigh (m) | 14,5 | 13,95 |
| Effective length (m) | 4 x 5 | 5 x 3,84 |
| Effective collecting area ($m^2$) | 34.800 | 89.994 |
| Type of discharge electrode | Spiral wire | Spiked wire |
| Number of electrodes per gas passage | 48 | 40 |
| Wire diameter (mm) | 2,7 | 5 (hydraulic) |

**Table 1. ESPs Geometry and Characterictics**

| | Series 1 | Series 2 | Series 3 | Series 4 |
|---|---|---|---|---|
| SCA (s/m) | 81,5 | 77,1 | 119,9 | 120,0 |
| Inlet dust conc. ($g/Nm^3$) | 22,0 | 24,7 | 11,7 | 13,0 |
| Dust resistivity (ohm.cm) | $4{,}10^{12}$ | $3{,}10^{11}$ | $3{,}10^{12}$ | $7{,}10^{11}$ |
| Gas temperature (ºC) | 116 | 125 | 128 | 122 |
| Voltage/Current density (kV)/($nA/cm^2$): | | | | |
| Field 1 | 38,8/1,0 | 61,6/11,9 | 42,0/19,0 | 40,5/21,8 |
| Field 2 | 33,5/0,9 | 63,2/15,9 | 45,5/8,0 | 41,8/16,8 |
| Field 3 | 31,5/0,5 | 40,0/3,3 | 43,5/9,8 | 40,8/16,5 |
| Field 4 | 29,8/0,3 | 40,0/2,5 | 44,0/14,2 | 42,8/18,2 |
| Field 5 | – | – | 43,0/2,5 | 40,3/19,4 |
| Voltage pulses: | | | | |
| Voltage (kV) | – | 56,0 | – | – |
| Duration ($\mu s$) | – | 125 | – | – |
| Frecuency (pps) | – | 5 | – | – |
| Avg. measured efficiency (%) | 94,62 | 99,93 | 99,66 | 99,72 |
| Avg. predicted efficiency (%): | | | | |
| PRELEC | 94,08 | 99,72 | 99,82 | 99,83 |
| EPA/SRI analysis | 75,00 | 98,25 | 99,87 | 99,88 |
| EPA/SRI design (*) | 98,70 | 99,00 | 99,91 | 99,90 |
| Avg. measured current density ($nA/m^2$) | 0,7 | 8,4 | 13,8 | 18,5 |
| Avg. predicted current density ($nA/m^2$): | | | | |
| PRELEC | 2,3 | 29,6 | 21,7 | 26,7 |
| EPA/SRI design (*) | 29,2 | 29,9 | 37,0 | 37,0 |

(*) Operation voltages are internally limited by model due to breakdown field limit.

**Table 2. Experimental Conditions and Global Model Results**

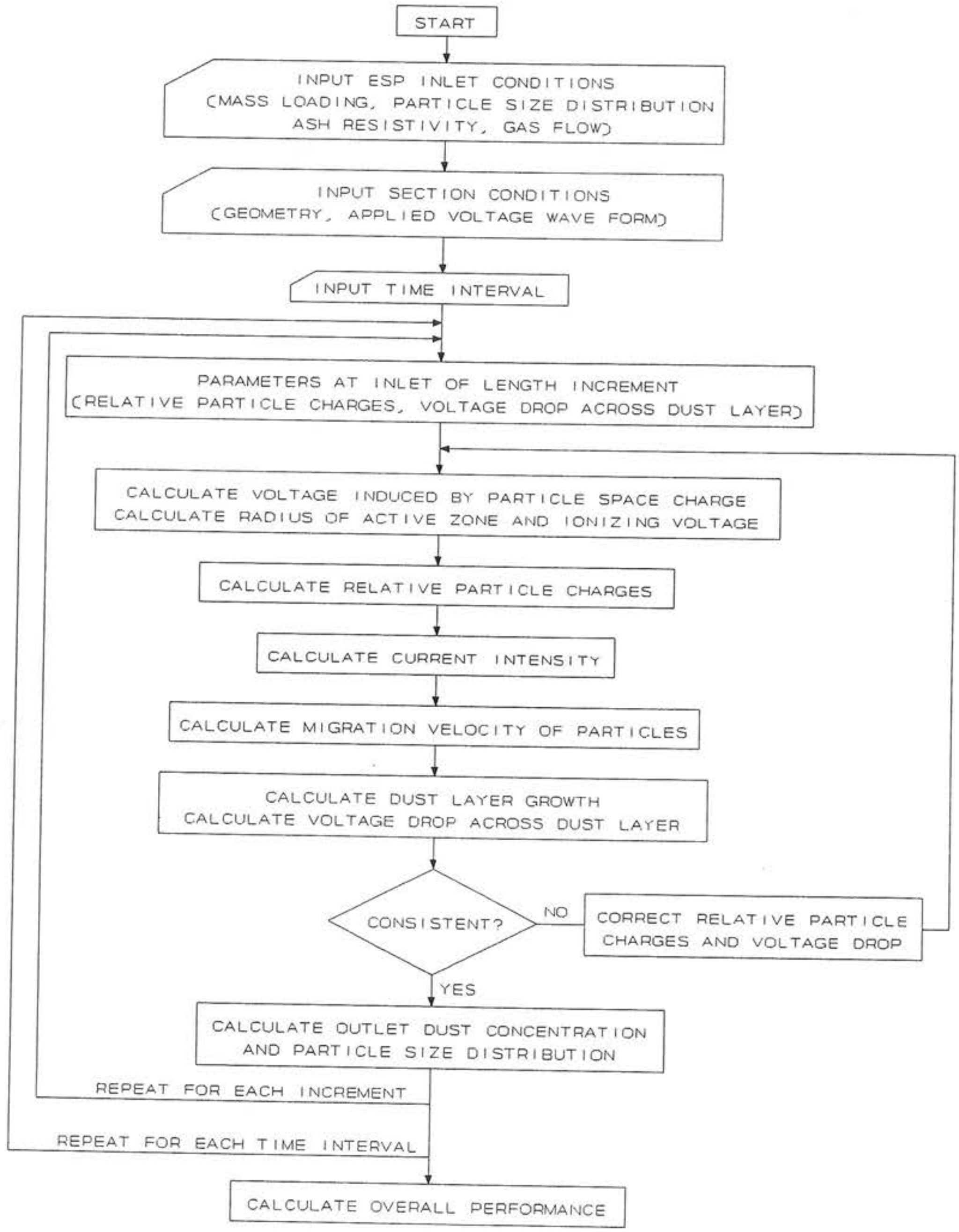


**Fig. 1. PRELEC Model Logic Diagram**

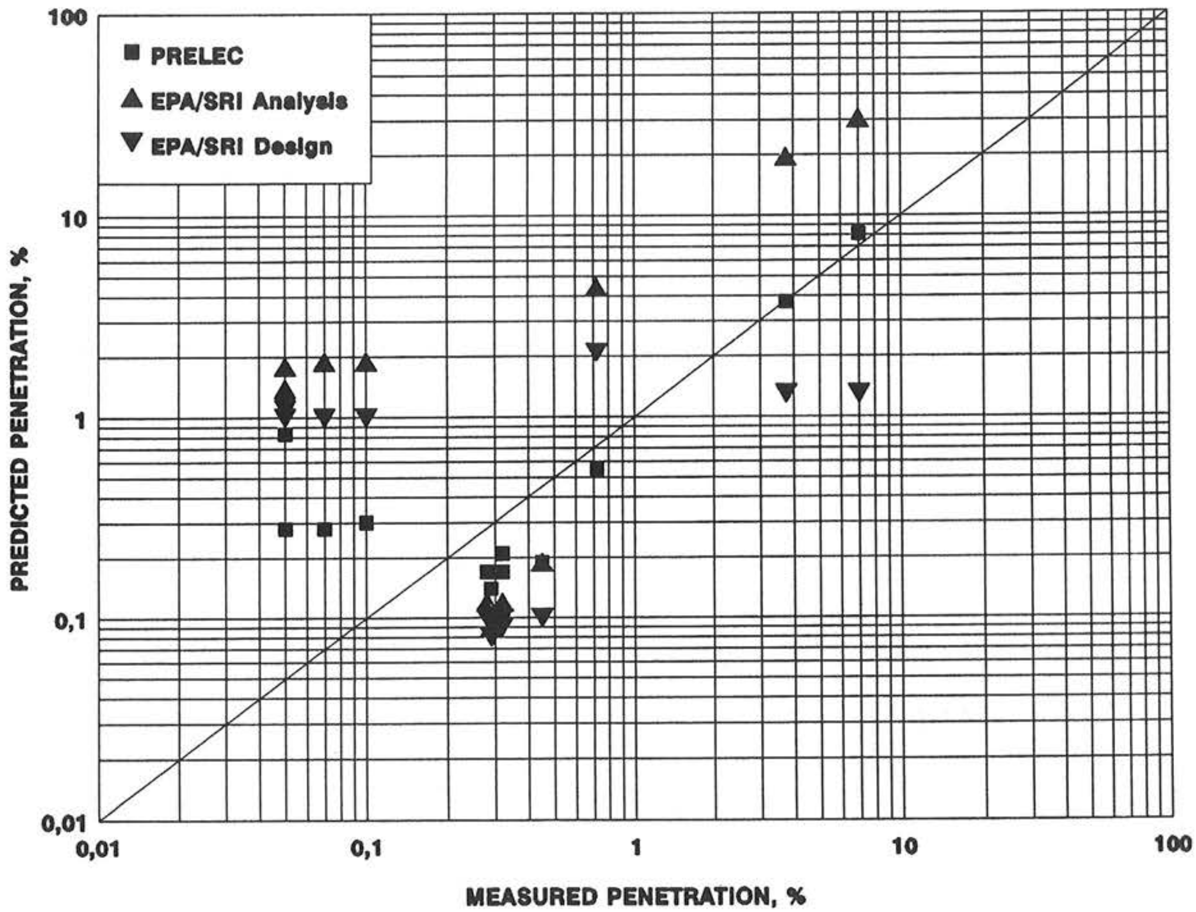


**Fig. 2. Measured ESP Penetration Compared with Model Penetration Calculations**

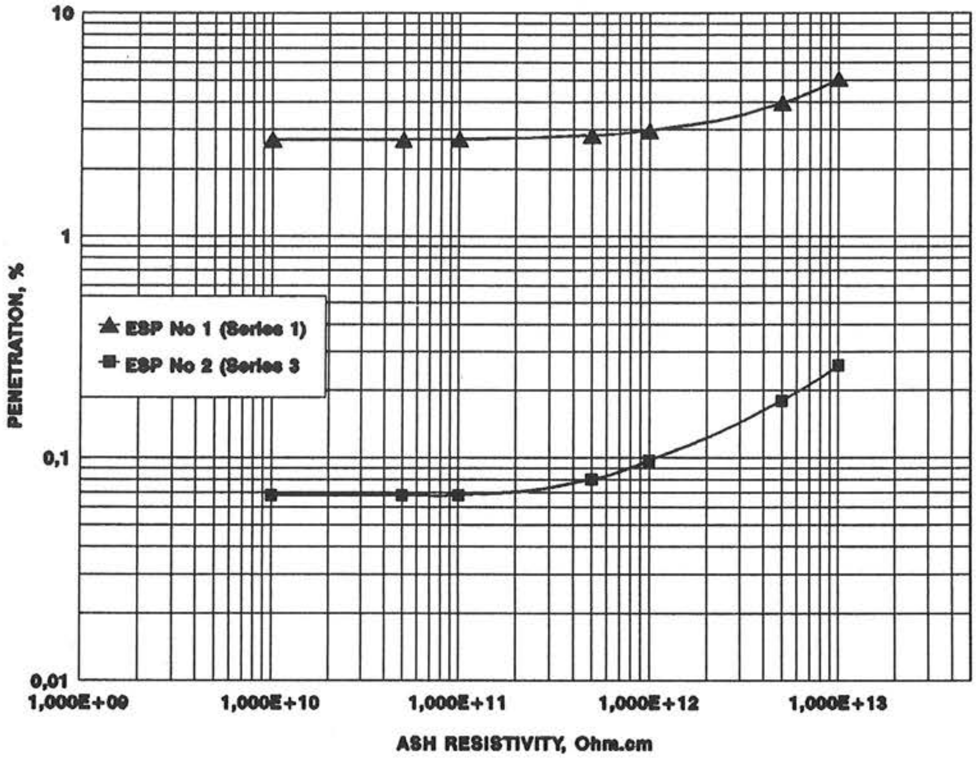


**Fig.3. Sensitivity of ESP Penetration to Resistivity**

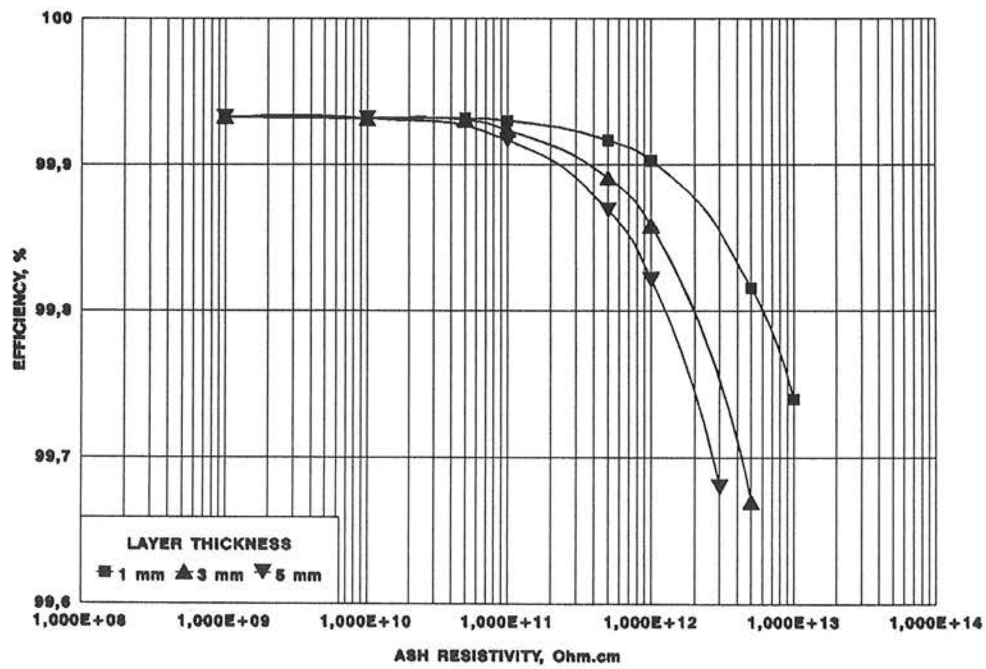


**Fig. 4. Sensitivity of ESP Efficiency to Dust Layer Thickness and Ash Resistivity**

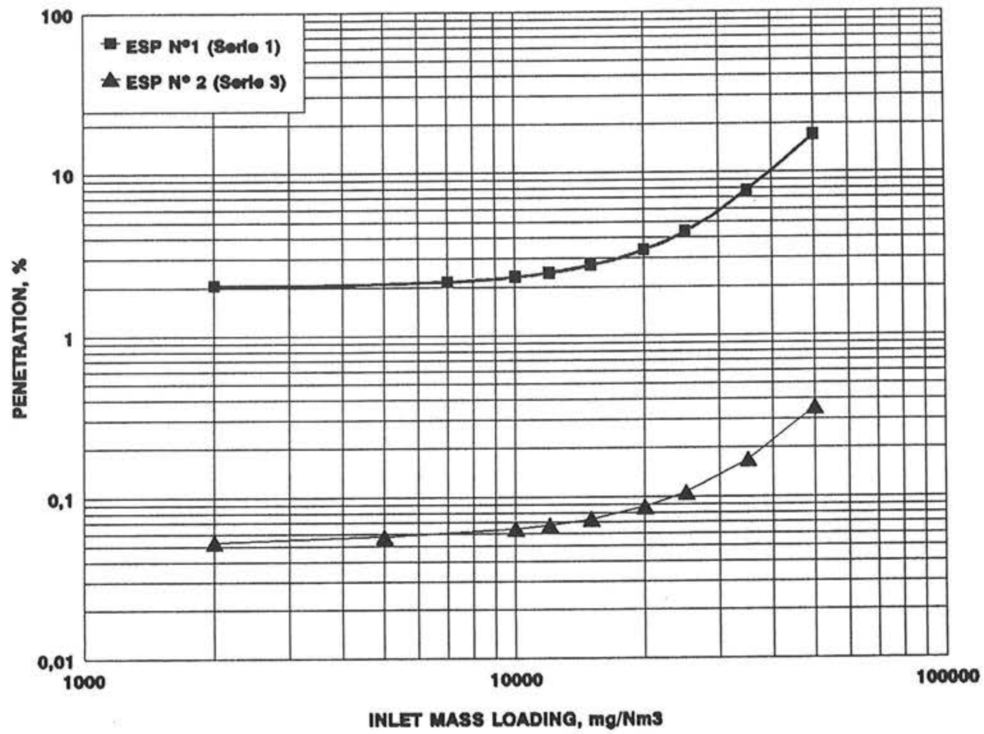


**Fig. 5. Sensitivity of ESP Penetration to Inlet Mass-Loading**

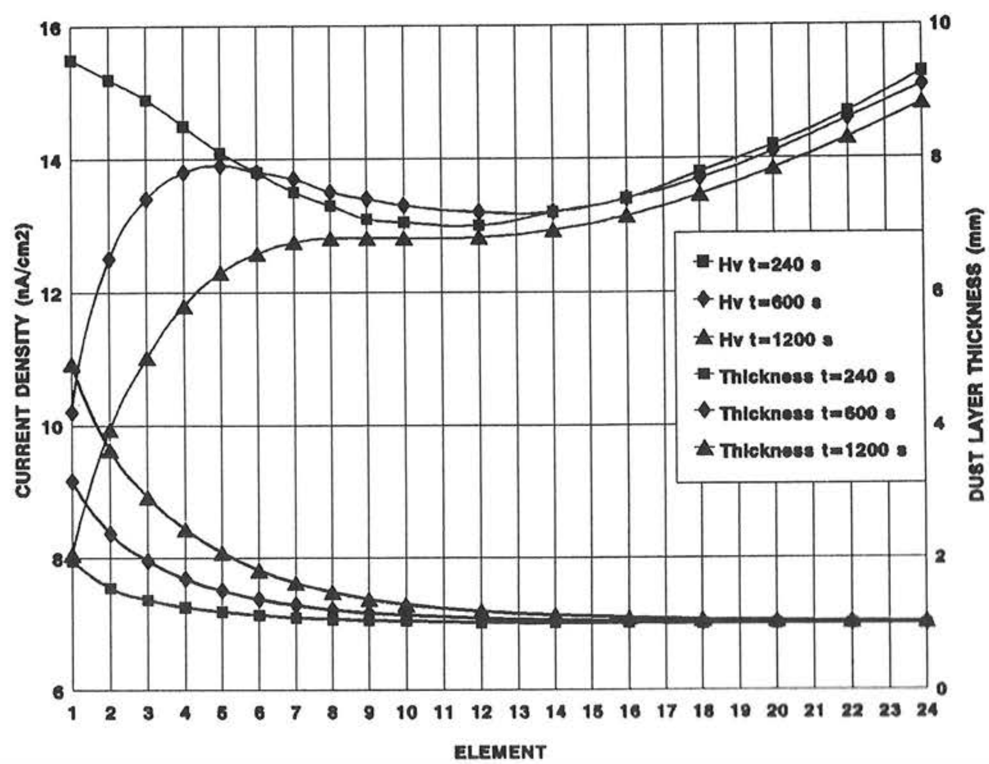


**Fig. 6. Transient Evolution of Current Density and Dust Layer Thickness**